Origin of Spectral Band Patterns in the Cosmic Unidentified Infrared Emission

Héctor Álvaro Galué[*]

Department of Physics and Astronomy, Vrije Universiteit, de Boelelaan 1081, 1081HV Amsterdam, Netherlands

Grisell Díaz Leines

Interdisciplinary Centre for Advanced Materials Simulation, Ruhr-Universität Bochum 44780 Bochum, Germany

The cosmic unidentified infrared emission (UIE) band phenomenon is generally considered as indicative of free-flying polycyclic aromatic hydrocarbon molecules in space. However, a coherent explanation of emission spectral band patterns depending on astrophysical source is yet to be resolved under this attribution. Meanwhile astronomers have restored the alternative origin as due to amorphous carbon particles, but assigning spectral patterns to specific structural elements of particles is equally challenging. Here we report a physical principle in which inclusion of nonplanar structural defects in aromatic core molecular structures (π domains) induces spectral patterns typical of the phenomenon. We show that defects in model π domains modulate the electronic-vibration coupling that activates the delocalized π-electron contribution to aromatic vibrational modes. The modulation naturally disperses $C = C$ stretch modes in band patterns that readily resemble the UIE bands in the elusive 6–9 μm range. The electron-vibration interaction mechanics governing the defect-induced band patterns underscores the importance of π delocalization in the emergence of UIE bands. We discuss the global UIE band regularity of this range as compatible with an emission from the delocalized sp^2 phase, as π domains, confined in disordered carbon mixed-phase aggregates.

Remarkably regular UIE band features appear typically on top of infrared (IR) emission plateaus of astrophysical sources [1] at 3.3, 6.2, 7.7, 8.6, and 11.2 μm (Fig. 1), with subtle band pattern variations depending on the source [2,3]. An illustrative band variation is the peak of the complex 7.7 μm band that changes from 7.8 μm in planetary nebulae to 7.6 μm in interstellar H II regions [Figs. 1(b) and 1(c)]. This implies structural differences between emission carriers in these two source types. Another key variation is the 6.2 μm band peak position that shifts $\leq 1.5\%$ [2,3].

As the UIE band patterns reveal the fingerprint of aromatic carbon [4], the carriers were early assigned to gas-phase, planar polycyclic aromatic hydrocarbons (PAHs) [5,6]. This interpretation uses spectra of hypothetical classes of PAHs to model the UIE bands [7–10], but cannot explain the origin of the band variations and PAH classes [11]. While this hinders the identification of specific structures, the PAH model is a working approximation to the vibrational mode signatures of photocooling UIE carriers heated by starlight [2,12]: the 6.2, 7.7, and 8.6 μm bands reveal $C = C$ stretch local-symmetry modes of (poly-)aromatic moieties, while the 3.3 and 11.2 μm bands reveal in-plane stretches and out-of-plane bends of aromatic C-H bonds [Fig. 1(d)]. The 7.7 and 8.6 μm bands also feature an in-plane C-H bend admixture. Clearly, H atoms are part of aromatic moieties. Minor UIE bands linked to nonaromatic C-H stretches at 3.4 and 6.9 μm show in diverse sources [13]. This so-called aliphatic emission suggests carriers made of polyaromatics linked by saturated

(sp^3) polymeric hydrocarbons [14,15], similar to the aromatic-aliphatic mixed composition of coal, petroleum fractions, and hydrogenated amorphous carbon [13–15]. These materials are robust models, but their suitability is doubted given the seemingly low content of aliphatic C relative to aromatic C ($\sim$0.09) estimated from the 3.3 and 3.4 μm UIE bands [16]. Whether the UIE carriers are free-flying planar PAHs or aromatic-aliphatic mixed particles is under debate [14,16].

In this Letter we use a molecular approximation to advance a physical origin of cosmic band patterns. We propose that the π delocalization behind the $C = C$ stretch IR activity of UIE bands is modulated by defects [17] in aromatic π-domain structures. This modulation can generate typical UIE band patterns as arising from the electron-vibration (vibronic) interaction mediated by π electrons. We evaluate absorption and emission IR properties of model π domains (Fig. 2) as a function of nonplanar defects by density functional theory and radiative IR cooling modeling (details in the Supplemental Material [18]), whereas the π-delocalization response to defects is studied via vibronic coupling phases [30]. These IR properties are determined by delocalized π electrons of aromatic sp^n hybridized orbitals [30,31], where $n = 2$ defines a planar composition, or $2 < n < 3$ an out-of-plane pyramidal composition [17]. Notably, defective out-of-plane structures are tridimensional and no longer fall under the standard chemical definition of PAHs. The structural transformations represented in Fig. 2 readily occur in
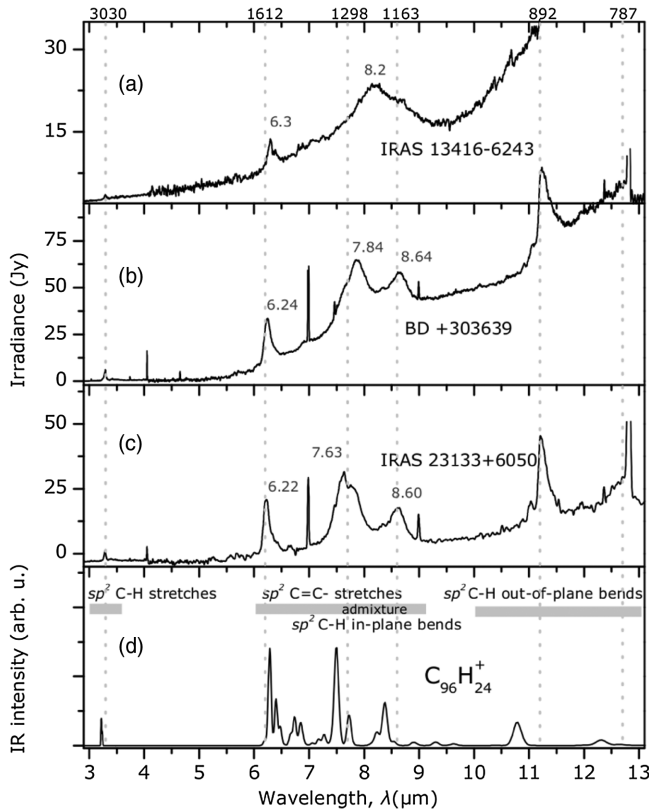
FIG. 1.   Observed IR spectra [1] of (a) protoplanetary and (b) planetary nebulae, and (c) an interstellar compact H II region. (d) Absorption spectrum of structurally intact, planar π domain [Fig. 2(a)]. The internal mode coordinates are labeled. Dotted lines: nominal frequencies (cm^{-1}) of UIE features.

polyaromatics, during ring formation in the growth phase [32] and photochemical decomposition [33,34]. Moreover, simulated astronomical carbon dust-grain analogues typically contain defective nonplanar π domains [35,36]. In circumstellar dust forming envelopes around evolved stars,

the photochemical processing of aliphatics in grains [37] can lead to a defective aromatization, and is implicated in the top-down formation of fullerenes [38–40]. We discuss π domains under disordered confinement as a necessary condition to explain the similar global spectral characteristics of UIE bands. This scenario suggests amorphous aggregates as main contributors to $C = C$ stretch UIE bands.

We calculate energy-minimum electronic structures and vibrational mode fundamental transitions (ν_k) of π domains via B3LYP/6-31G theory in Gaussian [43]. Line transitions in units of frequency ($\tilde{\nu}/cm^{-1}$) and IR oscillator strength ($A/10^3$ m mol^{-1}) are convoluted (15 cm^{-1} FWHM Lorentzian) and inserted in the photocooling model to obtain absorption and emission band spectra, respectively. Raw frequencies are scaled (0.965), which mitigates orbital-function truncation [18]. The adopted defect type is a peripheral pentagonal ring [17]. The benchmark model $C_{96}H_{24}^+$ in the charged cationic state is an intact π domain selected for its compact core structure found to contribute 18% to the irradiance of the source in Fig. 1(c) [8]. Only the cationic state is considered since neutral and anionic states add as little as 6.4% and 0.038% [8]. Note the size of this model ($L \approx 1.7$ nm) consistent with the average length (2 nm) of π-domain layers in laboratory cosmic grain analogues [35]. While other sizes are potentially relevant, we focus on the physics of delocalized IR activity and emission, and $C_{96}H_{24}^+$ is a suitable model. The related models $C_{95}H_{23}^+$, $C_{94}H_{22}^+$, and $C_{97}H_{21}^+$ are top-down structures with one, two, and three defects [17], which can also arise in bottom-up scenarios via acetylene ring-closure reactions at zigzag edges [32].

The delocalized IR activity is defined via the Born-Oppenheimer electronic wave function of a molecular π domain $\Psi_g(r; Q)$, r and Q being electron and nuclear coordinates [30,31]. On departure from the equilibrium
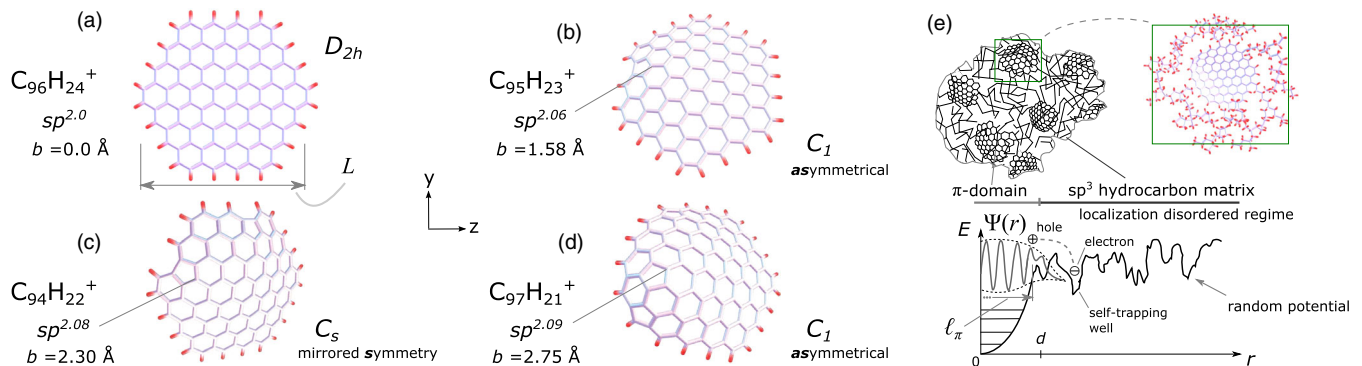
FIG. 2.   Molecular structures of H-terminated (red) π domains and grain aggregate model. (a) Planar nondefective π domain. Nonplanar π domains with defective pyramidal carbons as (b) one, (c) two, and (d) three pentagonal rings. Local hybridization sp^n (at highest pyramidal carbon) and global (bowl-depth b) curvature parameters are shown [17,18]. (e) Top: Schematic of amorphous two-phase aggregate with π domains (crystallite sp^2 phase) in insulating aliphatic matrix (disordered sp^3 phase) [41]. Bottom: Potential energy scheme $E(r)$ at crystallite-disorder interface [42], qualitative asymptotic behavior of domain's excited wave function $\Psi(r)$ and hole-electron charge separation due to ionization-induced self-trapped electron. The cationic (holelike) π-flux mode activation length ℓ_π is confined for $r < d$.

geometry Q_0 during vibration, Ψ_g can be expanded over equilibrium excited-state wave functions $\Psi_i(r, Q_0)$ that fit the π-electron density distortion: $\Psi_g = \Psi_o + \sum_i c_i \Psi_i$, Ψ_o being the ground state and $c_i = \langle \Psi_o | (\partial H / \partial Q_k)_0 | \Psi_i \rangle Q_k / \Delta E_{io}$. The matrix element is the Herzberg-Teller vibronic coupling strength, H the electronic Hamiltonian, Q_k the normal-mode coordinate, and ΔE_{io} the energy gap between excited and ground states. For distortions in charge separation states (e.g., due to ionization), π electrons migrate to typical low-lying unoccupied molecular orbitals π^* (intramolecular electron holes); these $\pi \rightarrow \pi^*$ excitations describe the states Ψ_i [30]. From the IR strength $A_k = N_A \pi / 3 c^2 \ln(10) (\partial \mu / \partial Q_k)^2$, where the electric dipole moment μ sums nuclear $\varrho_N(Q)$ and electronic $\langle \Psi_g | - er | \Psi_g \rangle$ parts, the dipole derivative $\partial \mu / \partial Q_k$ in terms of c_i is

$$\frac{\partial \mu}{\partial Q_k} \propto \sum_i \frac{\langle \Psi_o | (\partial H / \partial Q_k)_0 | \Psi_i \rangle}{\Delta E_{io}} \langle \Psi_o | r | \Psi_i \rangle, \qquad (1)$$

where $\langle \Psi_o | r | \Psi_i \rangle$ is the electronic transition matrix element. Equation (1) is the wavelike *charge-flux* term of IR activity by delocalized π electrons oscillating along Q_k.

We find a strong delocalized IR activity in $C_{96}H_{24}^+$ due to π fluxes across the bond-alternation z length, $\ell_\pi \approx L$. Specifically, selection rules reveal $C = C$ stretch antisymmetric b_{1u} modes featuring a long-range π flux mainly due to excited state $\Psi_e(^2B_{1g})$ mixing with $\Psi_o(^2A_u)$. The π flux

arises from the time-varying probability density of the one-electron excitation describing Ψ_e, and its vibronic coupling phases per mode determine its strength [Figs. 3(a) and 3(b)]. We consider two absorption bands due to b_{1u} modes ν_{214} and ν_{216} [Fig. 4(a)]. To evaluate their π-flux strength along the b_{1u}-mode coordinate of bond-alternation vibration [31] linking Q_0 geometries of Ψ_o and Ψ_e states, we compare their vibronic phases and intensities. So the π-flux strength ratio between ν_{214} and ν_{216} (6/4, Fig. 3) is approximately 16% lower than the IR strength ratio, $A_{214}/A_{216} = 1.8$. While this deviation likely reflects the unaccounted difference between ν_{214} and ν_{216} two-carbon centers, it is evident that ν_{214} acquires electronically a near twofold intensity enhancement.

Inclusion of nonplanar defects disrupts the mixed-in state Ψ_e. For π domains descending from $C_{96}H_{24}^+$ with one and two defects [Figs. 2(b) and 2(c)], we examine frontier π orbitals to map Ψ_e into Ψ_e^{as} in $C_{95}H_{23}^+$ and Ψ_e^s in $C_{94}H_{22}^+$; see Ref. [18]. The resultant time-varying probability densities generate partitioned π-electron density redistributions [see increasing one-carbon centers, Figs. 3(c) and 3(d)] yielding shorter range π fluxes along multiple modes, rather than an extended π flux as in ν_{214}.

An emerging property of asymmetrical defective non-planar π domains featuring medium- to short-range π fluxes is spectral substructure patterns. In Fig. 4, the spectra of defective π domains show emergent modes in all ν_{214}, ν_{232}, and ν_{239} ranges. For $C_{95}H_{23}^+$, pentagonal $C = C$ stretches
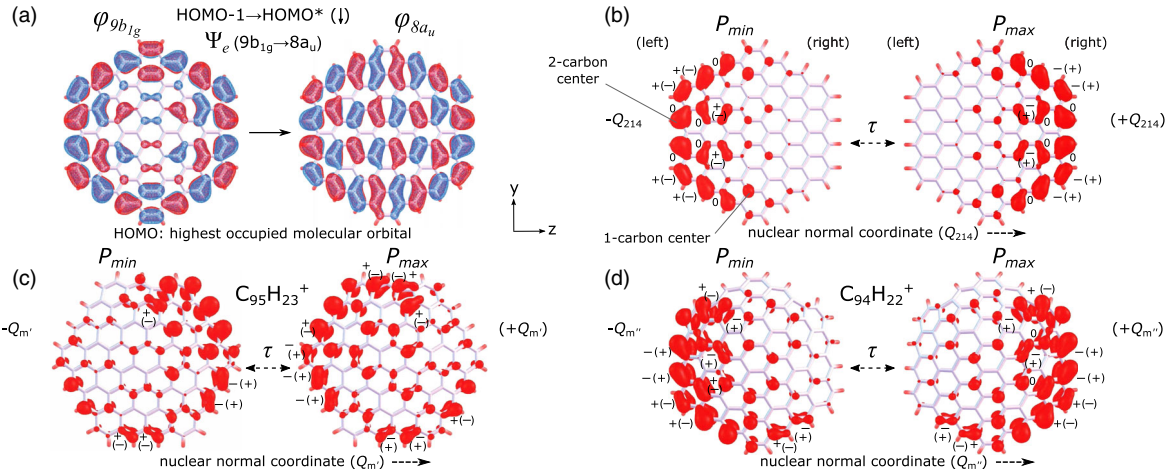
FIG. 3. Electronic π-delocalization source of IR activity. For $C_{96}H_{24}^+$, (a) one-electron $\pi(9b_{1g}) \rightarrow \pi^*(8a_u)$ orbital excitation describing mixed-in Ψ_e that activates $C = C$ stretch $b_{1u}(z)$ modes, and (b) dipolar delocalized π-electron flux. The π-electron density redistribution features minimum $P_{min} = (|\varphi_{9b_{1g}}| - |\varphi_{8a_u}|)^2$ and maximum $P_{max} = (|\varphi_{9b_{1g}}| + |\varphi_{8a_u}|)^2$ of time-varying probability density $P(r, t) = |\varphi_{9b_{1g}}(r) \exp(-iE_{9b_{1g}} t / \hbar) + \varphi_{8a_u}(r) \exp(-iE_{8a_u} t / \hbar)|^2$ and oscillation time $\tau = h / (E_{9b_{1g}} - E_{8a_u})$. Two-carbon π-electron centers maintain in-phase and out-of-phase relations with $C = C$ stretches at classical turning points of the b_{1u} modes. The vibronic coupling phases thus reveal induced stabilizing $(+)$ and destabilizing $(-)$ bond characters [30]. Phases along ν_{214} show a six-factor π-density accumulation in the left side relative to the right side (6 pairs $+, -$) at $-Q_{214}$ and vice versa [6 pairs $(-), (+)$] at $+Q_{214}$ creating a π flux across bond-alternation (activation) length ℓ_π. A four-factor defines the ν_{216} π-flux strength [18]. (c),(d) π fluxes along modes $\nu_{m'}$ and $\nu_{m''}$ of $C_{95}H_{23}^+$ and $C_{94}H_{22}^+$ (Fig. 4) from time-varying probability densities of mixed-in Ψ_e^{as} and Ψ_e^s. Vibronic coupling phases feature bond alternation among nearby rings, thus yielding shorter range π fluxes with y and/or x components. Molecular orbital wave functions $\varphi(r, Q_0)$ from electronic calculations.
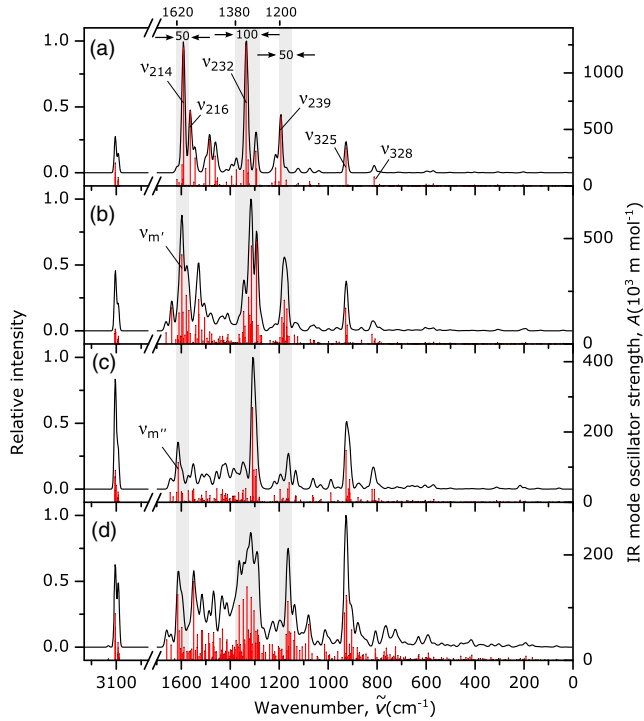
FIG. 4. Absorption IR spectra of (a) $C_{96}H_{24}^+$, (b) $C_{95}H_{23}^+$, (c) $C_{94}H_{22}^+$, and (d) $C_{97}H_{21}^+$. The $C = C$ stretch spectral ranges (gray) typified by b_{1u} modes ($\tilde{\nu}$; A) of $C_{96}H_{24}^+$: ν_{214} (1590; 1232), ν_{232} (1336; 1249), ν_{239} (1193; 613). The other dominant b_{1u} mode is ν_{216} (1563; 669). An in-plane C-H bend internal coordinate also describes ν_{232} and ν_{239}. The out-of-plane C-H bend $b_{3u}(x)$ modes ν_{325} and ν_{328} fall near 11.2 and 12.7 μm UIE bands [Fig. 1(d)]. Dominant ν_{214}-range modes of defective π domains are $\nu_{m'}$ (1598; 422) and $\nu_{m''}$ (1613; 113). The weak IR activity of low-frequency modes indicates a negligible π-flux term [Eq. (1)] at those energies.

keep effective bond-alternation phase relations with hexagonal $C = C$ stretches, suggesting sizable π-flux projections over modes. Along mode $\nu_{m'}$, these relations occur with rings at medium bond-alternation distance to the left [$+Q_{m'}$, Fig. 3(c)]. For $C_{94}H_{22}^+$, emergent modes are less IR active as justified by the lack of extended bond alternations. From the phases along $\nu_{m''}$ [Fig. 3(d)], couplings rather occur among adjacent rings, suggesting few emerging moderate modes which show as only one band per range on convolution. By simulating an extra defect, π fluxes decompose over more modes as suggested by the spectrum of the nonsymmetric π-domain $C_{97}H_{21}^+$ with higher curvature, increasing the spectral mode density [Fig. 4(d)]. Similarly to asymmetrical $C_{95}H_{23}^+$, the denser mode ranges disperse in patterns revealing a complex band in the ν_{232} range.

While even more defects can yield very complex spectra, we infer considering also previous work [17] a few-defects regime for compact π domains in which highly IR-active modes in the ν_{214} range tend to shift to higher frequencies, and to lower frequencies in the ν_{232} range (compare to $C_{96}H_{24}^+$ bands). In the ν_{239} range, dominant modes shift to
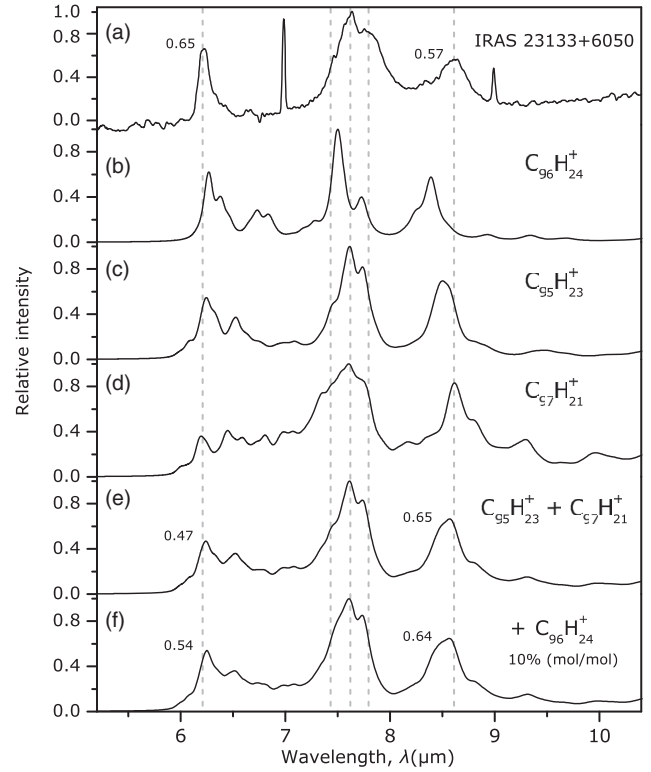
FIG. 5. Emission IR spectra of π domains and typical interstellar source in the $C = C$ stretch mode region. Relative intensity as emitted power density normalized to 7.7 μm band peak intensity: $S(\tilde{\nu}, T)/S_{7.7}$. Dependency on temperature of emission frequency $\tilde{\nu}(T)$ ($\rightarrow \lambda$) is modeled by the anharmonic spectral law of Ref. [45]. (a) Interstellar spectrum [Fig. 1(c)]. IR photocooling after 10 eV excitation for (b) $C_{96}H_{24}^+$ at peak temperature 792 K, (c) $C_{95}H_{23}^+$ at 801 K, and (d) $C_{97}H_{21}^+$ at 799 K. Average emissions from (e) $C_{95}H_{23}^+$ and $C_{97}H_{21}^+$ (1:1), and (f) $C_{95}H_{23}^+$, $C_{97}H_{21}^+$ and $C_{96}H_{24}^+$ (0.45: 0.45: 0.10).

lower frequencies. Whereas these spectral trends may be seen as a symmetry lowering effect, the lack of relevant band patterns, while going from compact to irregular planar structures [44], shows the unique effect of defect-induced curvature on spectra via the π-flux term. In Fig. 4, this term does not stem from an explicit Herzberg-Teller wave function approach, but the electronic exchange-correlation contribution to B3LYP energy functional [30].

Figure 5 shows direct comparisons between the IR photocooling spectra of π domains $S(\tilde{\nu}, T)$ [Eq. (2) in Ref. [18]] after peak temperature excursions, and the spectrum in Fig. 1(c) taken as representative of interstellar UIE bands. From Fig. 4, we anticipate that IR properties of defective π domains are well embodied in the interstellar emission. Contrary to the emission pattern of the planar structure [Fig. 5(b)], the defect-induced mode dispersion yields band patterns reproducing the three-component profile of the 7.7 μm band and nominal positions of 6.2 and 8.6 μm bands [Figs. 5(c) and 5(d)]. Moreover, the average emission [Fig. 5(e)] suggests that interstellar UIE

carriers consist of π-domain structures with a diverse number of defects. Assuming that carriers are grain aggregates with an aromatic sp^2-carbon phase of $C_{95}H_{23}^+$ and $C_{97}H_{21}^+$ in a 1:1 ratio, the 6.2 μm band [Fig. 5(a)] reflects blended spectral components which reveal defective (pyramidal) structural properties typical of both π domains. It is conceivable that a fraction of the interstellar aggregate sp^2 phase involves planar π domains. Figure 5(f) shows this case with average adding 10 mol% of $C_{96}H_{24}^+$. The intensity of the average 6.2 μm band raises to 0.54 whereas at 6.5 μm it fades out. This shows that planar π domains [8] contribute to the delocalized sp^2 phase of carriers.

The implied evolution of UIE band patterns along structural curvature b (including $b = 0$) is congruent with the IR fingerprint of laboratory cosmic grain analogues, where $C = C$ stretch bands indicate the tridimensional shapes of constituent π domains [36]. From an atomistic perspective, the band pattern variations reflect the transitional pyramidal composition between aromatic (sp^2) and aliphatic (sp^3) bonds. The defect-curvature driven modulation of π-flux activated modes in aromatic structures thus generates the global UIE band profile and variations.

An open question is whether structures occur in the gas phase or as part of grains. Contrary to grains, it is argued that only gas-phase PAHs can be excited to temperatures required for IR emission due to their smaller size [7]. However, we have shown that UIE band patterns arise from modulations of the delocalized π-flux mode activation. So enforcing this energetic argument implies that astronomical PAHs must feature unique planar shapes to generate the universal profile of UIE bands, since free PAH wave functions have a full edge-topology character manifested in the π flux [30]. In other words, the more irregularly shaped the PAH is, the more irregular its spectrum looks [44]. Observational efforts have indeed shown the absence of unique PAHs in space [46], pointing toward structures in grains.

In our aggregate model of π domains in a sp^3 phase disorder [Fig. 2(e)], the loss of electronic coherence inherent to the confined π flux can explain the UIE band regularity. An excited π-domain electronic wave function $\Psi(r)$, essentially defining the characteristic delocalized π-flux mode activation length ℓ_π, has a nonzero probability of backscattering at surrounding irregular sites plus a tunneling probability [47]. Both probabilities disrupt the wave function phase coherence ϕ, which is arguably more pronounced at the domain-disorder interface ($r \approx d$). At low temperature and depending on the π-domain spatial orientation, these quantum interferences can reduce the transmission wave amplitude [47] yielding a π flux surviving within the coherence length $\ell_\pi \leq \ell_\phi \sim d$. So regardless of the edges of an embedded π domain, a corelike coherence-limited π flux implies regular $C = C$ stretch IR emissions.

Disordered confinement further suggests conditions of thermal insulation [41]. In this scenario, photoionization

of embedded π domains produces charge-separation states [42,48], of which the eventual photoexcitation and emission [Figs. 5(b)–5(f)] are hence described within the molecular approximation. Other sources of charge separation such as chemical impurities (e.g., heteroatoms) [49] could play a role.

---

[*]h.alvarogalue@gmail.com

[1] G. C. Sloan, K. E. Kraemer, S. D. Price, and R. F. Shipman, Astrophys. J. Suppl. Ser. **147**, 379 (2003).

[2] K. Sellgren, Spectrochim. Acta Mol. Biomol. Spectrosc. **57**, 627 (2001).

[3] E. Peeters, S. Hony, C. Van Kerckhoven, A. G. G. M. Tielens, L. J. Allamandola, D. M. Hudgins, and C. W. Bauschlicher, Astron. Astrophys. **390**, 1089 (2002).

[4] W. W. Duley and D. A. Williams, Mon. Not. R. Astron. Soc. **196**, 269 (1981).

[5] A. Léger and J. L. Puget, Astron. Astrophys. **137**, L5 (1984).

[6] L. J. Allamandola, A. G. G. M. Tielens, and J. R. Barker, Astrophys. J. **290**, L25 (1985).

[7] A. Tielens, Annu. Rev. Astron. Astrophys. **46**, 289 (2008).

[8] A. Ricca, C. W. Bauschlicher, C. Boersma, A. G. G. M. Tielens, and L. J. Allamandola, Astrophys. J. **754**, 75 (2012).

[9] M. J. F. Rosenberg, O. Berné, and C. Boersma, Astron. Astrophys. **566**, L4 (2014).

[10] H. Andrews, C. Boersma, M. W. Werner, J. Livingston, L. J. Allamandola, and A. G. G. M. Tielens, Astrophys. J. **807**, 99 (2015).

[11] Y. Zhang and S. Kwok, Astrophys. J. **798**, 37 (2015).

[12] K. Sellgren, Astrophys. J. **277**, 623 (1984).

[13] G. C. Sloan, M. Jura, W. W. Duley, K. E. Kraemer, J. Bernard Salas, W. J. Forrest, B. Sargent, A. Li, D. J. Barry, C. J. Bohac et al., Astrophys. J. **664**, 1144 (2007).

[14] S. Kwok and Y. Zhang, Nature (London) **479**, 80 (2011).

[15] F. Cataldo, D. A. Garca-Hernández, and A. Manchado, Mon. Not. R. Astron. Soc. **429**, 3025 (2013).

[16] A. Li and B. T. Draine, Astrophys. J. Lett. **760**, L35 (2012).

[17] H. Alvaro Galué, Chem. Sci. **5**, 2667 (2014).

[18] See Supplemental Material at http://link.aps.org/supplemental/10.1103/PhysRevLett.119.171102 for details in methodology, which includes Refs. [19–29].

[19] A. D. Becke, J. Chem. Phys. **98**, 5648 (1993).

[20] M. H. Stockett, H. Zettergren, L. Adoui, J. D. Alexander, U. Bēziņš, T. Chen, M. Gatchell, N. Haag, B. A. Huber, P. Hvelplund et al., Phys. Rev. A **89**, 032701 (2014).

[21] H. Alvaro Galué, C. A. Rice, J. D. Steill, and J. Oomens, J. Chem. Phys. **134**, 054310 (2011).

[22] W. W. Duley and D. A. Williams, Mon. Not. R. Astron. Soc. **231**, 969 (1988).

[23] A. C. Ferrari and J. Robertson, Phys. Rev. B **61**, 14095 (2000).

[24] R. E. Smalley, Annu. Rev. Phys. Chem. **34**, 129 (1983).

[25] W. W. Duley and D. A. Williams, Astrophys. J. Lett. **737,** L44 (2011).

[26] C. Pech, C. Joblin, and P. Boissel, Astron. Astrophys. **388,** 639 (2002).

[27] J. Oomens, A. G. G. M. Tielens, B. G. Sartakov, G. von Helden, and G. Meijer, Astrophys. J. **591,** 968 (2003).

[28] A. Candian and P. J. Sarre, Mon. Not. R. Astron. Soc. **448,** 2960 (2015).

[29] N. L. Martín-Hernández, E. Peeters, C. Morisset, A. G. G. M. Tielens, P. Cox, P. R. Roelfsema, J.-P. Baluteau, D. Schaerer, J. S. Mathis, F. Damour *et al.*, Astron. Astrophys. **381,** 606 (2002).

[30] H. Alvaro Galué, J. Oomens, W. J. Buma, and B. Redlich, Nat. Commun. **7,** 12633 (2016).

[31] H. Torii, J. Mol. Struct. **1056,** 84 (2014).

[32] R. Whitesides and M. Frenklach, J. Phys. Chem. A **114,** 689 (2010).

[33] A. J. de Haas, J. Oomens, and J. Bouwman, Phys. Chem. Chem. Phys. **19,** 2974 (2017).

[34] P. Parneix, A. Gamboa, C. Falvo, M. Bonnin, T. Pino, and F. Calvo, Mol. Astrophys. **7,** 9 (2017).

[35] C. Jäger, F. Huisken, H. Mutschke, I. L. Jansa, and T. Henning, Astrophys. J. **696,** 706 (2009).

[36] Y. Carpentier, G. Féraud, E. Dartois, R. Brunetto, E. Charon, A.-T. Cao, L. D'Hendecourt, P. Bréchignac, J.-N. Rouzaud, and T. Pino, Astron. Astrophys. **548,** A40 (2012).

[37] A. P. Jones, L. Fanciullo, M. Köhler, L. Verstraete, V. Guillet, M. Bocchio, and N. Ysard, Astron. Astrophys. **558,** A62 (2013).

[38] D. A. García-Hernández, A. Manchado, P. García-Lario, L. Stanghellini, E. Villaver, R. A. Shaw, R. Szczerba, and J. V. Perea-Calderón, Astrophys. J. Lett. **724,** L39 (2010).

[39] D. A. García-Hernández, E. Villaver, P. García-Lario, J. A. Acosta-Pulido, A. Manchado, L. Stanghellini, R. A. Shaw, and F. Cataldo, Astrophys. J. **760,** 107 (2012).

[40] E. R. Micelotta, A. P. Jones, J. Cami, E. Peeters, J. Bernard-Salas, and G. Fanchini, Astrophys. J. **761,** 35 (2012).

[41] J. D. Carey and S. R. P. Silva, Phys. Rev. B **70,** 235417 (2004).

[42] M. Orrit, Photochem. Photobiol. Sci. **9,** 637 (2010).

[43] M. J. Frisch, G. W. Trucks, H. B. Schlegel, G. E. Scuseria, M. A. Robb, J. R. Cheeseman, G. Scalmani, V. Barone, B. Mennucci, G. A. Petersson *et al.*, Gaussian 09, Revision A.02 (2009).

[44] C. W. Bauschlicher, E. Peeters, and L. J. Allamandola, Astrophys. J. **697,** 311 (2009).

[45] D. J. Cook and R. J. Saykally, Astrophys. J. **493,** 793 (1998).

[46] G. C. Clayton, K. D. Gordon, F. Salama, L. J. Allamandola, P. G. Martin, T. P. Snow, D. C. B. Whittet, A. N. Witt, and M. J. Wolff, Astrophys. J. **592,** 947 (2003).

[47] C. Kittel, *Introduction to Solid State Physics* (Wiley, New York, 2005).

[48] T. Heitz, C. Godet, J. Bourée, B. Drévillon, and J. P. Conde, Phys. Rev. B **60,** 6045 (1999).

[49] A. C. Ferrari, S. E. Rodil, and J. Robertson, Phys. Rev. B **67,** 155306 (2003).